



Science Arts & Métiers (SAM)

is an open access repository that collects the work of Arts et Métiers Institute of Technology researchers and makes it freely available over the web where possible.

This is an author-deposited version published in: <https://sam.ensam.eu>
Handle ID: <http://hdl.handle.net/10985/19662>

To cite this version :

Jinyang XU, Chao LI, Ming CHEN, Fei REN, Mohamed EL MANSORI - An investigation of drilling high-strength CFRP composites using specialized drills - International Journal of Advanced Manufacturing Technology - Vol. 103, n°9-12, p.3425-3442 - 2019

Any correspondence concerning this service should be sent to the repository

Administrator : scienceouverte@ensam.eu



An investigation of drilling high-strength CFRP composites using specialized drills

Jinyang Xu¹ · Chao Li¹ · Ming Chen¹ · Mohamed El Mansori^{2,3} · Fei Ren⁴

Abstract

Machining of high-strength carbon fiber reinforced polymers (CFRPs) has faced great challenges in quality control and tool wear management due to their inherent heterogeneity and high abrasiveness leading to serious workpiece damage and rapid tool wear. The present paper contributes to an experimental investigation of evaluating the machinability of one type of high-strength T800/X850 CFRPs representative of aircraft components. The novelty of this work lies in identifying the effects of different specialized drills on the drilling process of the high-strength CFRPs by covering a variety of aspects involving the drilling forces, hole morphologies, workpiece damage, hole dimensional accuracy, and tool wear. Both the in-situ and post-process measuring results were correlated with the input process parameters and the used drill bits. A particular focus was placed on the inspections of the resulting tool morphologies and wear mechanisms governing the drilling of the high-strength CFRPs. The results highlight the importance of using functionally designed drills and optimum cutting conditions in realizing the damage-free drilling of T800/X850 composites.

Keywords High-strength CFRP composites · Drilling · Specialized drills · Drilling-induced damage · Hole quality · Tool wear

1 Introduction

Carbon fiber reinforced polymer (CFRP) composites are being extensively used for various lightweight constructions in the aerospace, automotive, and energy sectors due to their superior mechanical/physical properties [1–3]. This can be evidenced by the huge application potentials of CFRP starting with the Airbus A380 and a wider use of composites in the Boeing 787 Dreamliner. The CFRP families can be classified into three categories involving low-strength, high-strength,

and S-type CFRPs according to the mechanical properties of reinforcing fibers. High-strength CFRP composites which are typically reinforced by T800 grade fibers become very attractive in the applications of main load-carrying structures of large passenger aircraft, being an alternative to low-strength CFRPs and S-type CFRPs because of their much higher mechanical characteristics. However, this type of CFRP possesses extremely poor machinability, facing great challenges in quality control and tool wear management when subjected to a machining process.

Although most CFRP parts are fabricated roughly in a near-net shape, secondary machining processes such as drilling and milling are still required to meet the final design specifications. Machining of fibrous composites, particularly drilling, is being extensively used to produce riveted and bolted joints for the post assembly operations. However, the unique properties of CFRPs like the stiff and abrasive carbon fibers and the heat-sensitive matrix make the drilling process more challenging and expensive. In drilling CFRP composites, rapid tool wear is a characteristic phenomenon widely overserved due to the highly abrasive nature of carbon fibers and the low thermal conductivity of the carbon/epoxy system. The anisotropic and heterogeneous architecture of the composite combined with the excessive tool wear makes it likely

✉ Jinyang Xu
xujinyang@sjtu.edu.cn

¹ State Key Laboratory of Mechanical System and Vibration, School of Mechanical Engineering, Shanghai Jiao Tong University, Shanghai 200240, People's Republic of China

² MSMP – EA 7350, Arts et Métiers ParisTech, 51006 Châlons-en-Champagne, France

³ Department of Mechanical Engineering, Texas A&M University, College Station, TX 77840, USA

⁴ Shanghai Aerospace Equipments Manufacturer Co., Ltd., Shanghai 200245, People's Republic of China

to induce critical subsurface damage in the workpiece in a variety of forms including delamination, fiber pullouts, cracking, fuzzing, spalling, and matrix sintering or burning. Apart from the issues of serious damage and poor hole quality following the drilling of CFRP materials, rapid tool wear associated with various drill geometries and materials is also a critical concern among manufacturing sectors since it directly affects the effective control of hole quality and machining costs. In recent years, different tool materials including high-speed steel (HSS), carbides, coated HSS, coated carbides, and diamond-coated carbides have been examined to understand the wear mechanisms for managing and enhancing the tool life during drilling conventional low-strength CFRPs. Most of the research works carried out to assess the performance of these drill materials have identified abrasive wear as one of the major wear mechanisms [4–7]. In ref. [4], Malhotra reported the occurrence of both chisel edge wear and flank wear during the drilling of carbon/epoxy composites with HSS and carbide drills under the conditions of relatively low spindle speeds and feed rates. Rawat and Attia [5] found that the abrasive wear of WC drills resulting from drilling woven CFRPs is the consequences of both hard and soft abrasion modes. The authors highlighted that chipping and abrasion were the main mechanisms controlling the deterioration of WC drills. In the light of the widely observed abrasion wear in drilling fibrous composites, Faraz et al. [6] proposed a new wear criterion termed as the cutting edge rounding (CER) for the quantification of wear extents of uncoated carbide tools during the drilling of CFRP composites. A series of experimental tests using different types of drills were conducted which confirmed the applicability of this new wear feature in assessing the severity of tool wear. Wang et al. [7] studied the wear patterns of various coated drills when drilling CFRPs and found that the diamond coating could significantly reduce the edge rounding wear while the AlTiN coating failed to protect the drill due to its oxidation during machining. In spite of the aforementioned well-performed studies, investigations concerning the wear behavior and cutting performances of specialized drills in drilling high-strength CFRPs are very limited.

To date, a large number of experimental studies have been conducted to better understand the correlations between process inputs, such as machining parameters and drill geometries, and process outputs such as cutting forces, tool wear, and hole quality. For instance, Shyha et al. [8] investigated the effects of drill geometries and operating parameters when drilling small diameter holes in CFRP materials. The authors found that both the drill type and the feed rate were the key factors affecting the tool life and the thrust force, while the cutting speed and the feed rate had the most significant effect on the torque. Karpat et al. [1] addressed the drilling machinability of thick fabric woven CFRP laminates by using different types of point angle drills. The results indicated that

delamination in fabric woven CFRP laminates was closely associated with the conditions of the diamond coating. Peak thrust forces are observed to increase significantly as a result of fracturing of the diamond coating. Hole diameter tolerance became more critical than hole exit delamination during the drilling of fabric woven CFRP laminates. Sorrentino et al. [9] studied the extents of peel-up and push-out delamination when drilling CFRP composites. Based on the identification of harmful sets of cutting parameters, the authors proposed the variable feeding method to reduce the delamination damage of fibrous composites and found that the use of the new drilling method could reduce the push-out delamination factor by 37% for the CFRP material. Loja et al. [10] carried out an assessment of thermally influenced and delamination-induced regions during the drilling of fibrous composites. It was found that the tool geometries and the thickness of the workpiece were the key factors affecting significantly the drilling-induced damage of the composite laminates. Fernández-Pérez et al. [11] studied the influences of process parameters on the tool wear and hole quality while drilling aerospace grade composite materials. The authors found that edge chipping and abrasive wear were the key wear modes dominating the drilling of fibrous composites and the wear extent had a great impact on the quality of drilled holes. Additionally, Díaz-Álvarez et al. [12] presented an experimental analysis of the drilling damage for aramid composites using different drill geometries and cutting parameters. It was found that fuzzing as well as delamination was the dominant damage mechanisms in most cases and the brad spur drill generally yielded the best performance in achieving good hole quality. Qiu et al. [13] evaluated the feasibility of one conventional twist drill and three step drills differing in the ratio of primary drill diameter to secondary drill diameter (k) for drilling CFRP composites. Results showed that high spindle speeds favored the chisel edge to remove the carbon fibers toward the exit side and the step drill with a k parameter equal to 0.5 produced the best exit hole quality even in the case of using large processing parameters. Recently, Geier et al. [14] analyzed the influence of a non-conventional drilling direction on the hole quality and thrust force for conventional CFRP materials. The results showed that the cutting speed has a more significant impact when drilling UD-CFRP at the non-conventional drilling direction than at the conventional one and the specific feed force in the non-conventional drilling direction was more than three times higher than that in the conventional one. Moreover, several review articles dealing with the drilling of CFRP composites are given in the open literature [15, 16].

Despite the availability of the abovementioned contributions, there still exist very few works dealing with the drilling of high-strength CFRPs. The present work is thus aimed at contributing to an experimental investigation into the drilling characteristics of high-strength T800/X850 CFRPs representative of aircraft components. The novelty of this work lies in

identifying the feasibility of using different specialized drills in improving the machinability of the high-strength CFRP. The results discussed in this paper could add knowledge to the machining field of high-strength CFRPs and contribute to the scientific understanding of the correlations between the process parameters and the drilling responses, which can guide the composite applications in the modern aerospace industry.

2 Experimental procedures

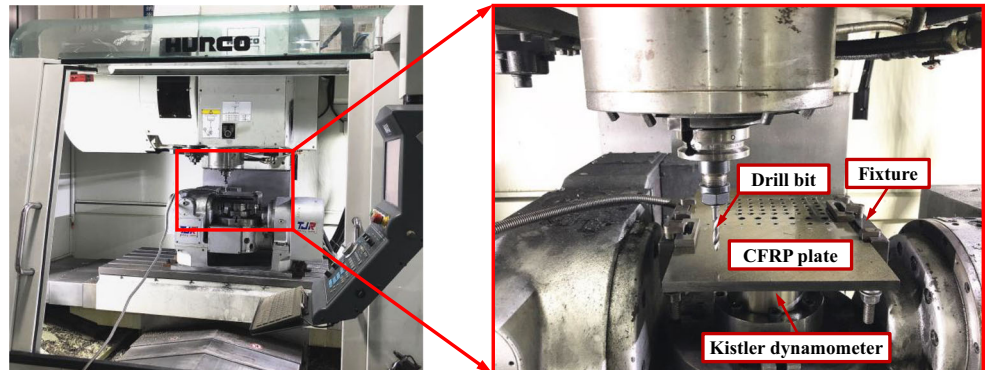
The drilling studies were performed without coolants on a HURCO VMX42 CNC machining center as shown in Fig. 1. The test specimens are multidirectional carbon/epoxy laminates constituted by high-strength T800 fibers and X850 resin matrix, which have a total thickness of 9.16 mm consisting of 48 plies subjected to the $[(45^\circ/90^\circ/-45^\circ/0^\circ)_6]_s$ stacking sequence as depicted in Fig. 2.

During the drilling tests, the CFRP plate was firmly clamped by a specially designed fixture mounted on a piezoelectric dynamometer (Kistler 9272). The dynamometer was equipped with a multichannel charge amplifier (Kistler 5070A) and a data acquisition system allowing the in-situ measurement of the drilling forces at an acquisition frequency of 20 kHz. To finalize the high-strength CFRP drilling process, three types of drills differing in geometrical features with an identical diameter equal to 6.35 mm were adopted as shown in Fig. 3. The first tool is a CVD diamond-coated brad spur drill characterized by two protruding edges at the drill periphery specializing in cutting off carbon fibers with a point angle of 118° and a helix angle of 38° . The second and third tools are respectively an uncoated tungsten carbide twist drill featured by a point angle of 140° and a helix angle of 35° and an uncoated solid carbide dagger drill offered by Sandvik Coromant. The dagger drill is characterized by a $118^\circ \times 25^\circ$ two-stage point design with a corresponding helix angle of 10° and a 64.89 mm length of chip flute (LCF). The drill consists of four straight flutes that are

recommended for the quick evacuation of chips as depicted in Fig. 3c. Another key characteristic of the dagger drill is the web, which comes to a point for decreasing the thrust force while drilling. To identify the parametric effects on the drilling outputs of high-strength CFRPs, a full factorial experimental design consisting of four levels for the spindle speed ($n = 1000, 1500, 2000, 2500$ rpm) and four levels for the feed rate ($f = 0.010, 0.015, 0.020, 0.025$ mm/rev) was adopted according to the recommendations by the workpiece supplier. Note that the magnitudes of the drilling parameters used herein were lower than those commonly used in drilling conventional CFRPs in order to minimize the damage extents of the high-strength CFRP workpiece. Table 1 shows the details of the experimental conditions designed for the drilling of T800/X850 laminates. For each set of cutting parameters, three test repetitions were conducted in order to ensure the reliable measurements of the drilling results.

After the completion of the drilling tests, the morphologies of CFRP hole surfaces produced by various drill bits were characterized via a TESCAN MIRA3 scanning electron microscope (SEM). The interlaminar delamination commonly occurring among adjacent plies inside the interior of a CFRP laminate was detected by a high-frequency KSI v-400E scanning acoustic microscope (SAM), which is a non-destructive diagnostic system widely used for failure analysis, process, and quality control applications. To accurately quantify the extents of interlaminar delamination, a new evaluation factor, namely the three-dimensional delamination factor (F_v), was utilized in the present work which is defined as the ratio of the cumulative volume (V_d) to the nominal hole volume (V_{nom}) of delaminated composite layers. Regarding the full details of the characterizing process of the interlaminar delamination using the SAM equipment and the calculations of the three-dimensional delamination factor, readers are directed to the work done by Xu et al. [17]. Additionally, diameters of hole surfaces with locations at 1 mm beneath the hole entry side, 1 mm over the hole exit side, and at the hole middle side were measured by a SOLEX EUA coordinate measuring machine (CMM).

Fig. 1 Experimental setup for the drilling of high-strength CFRP composites



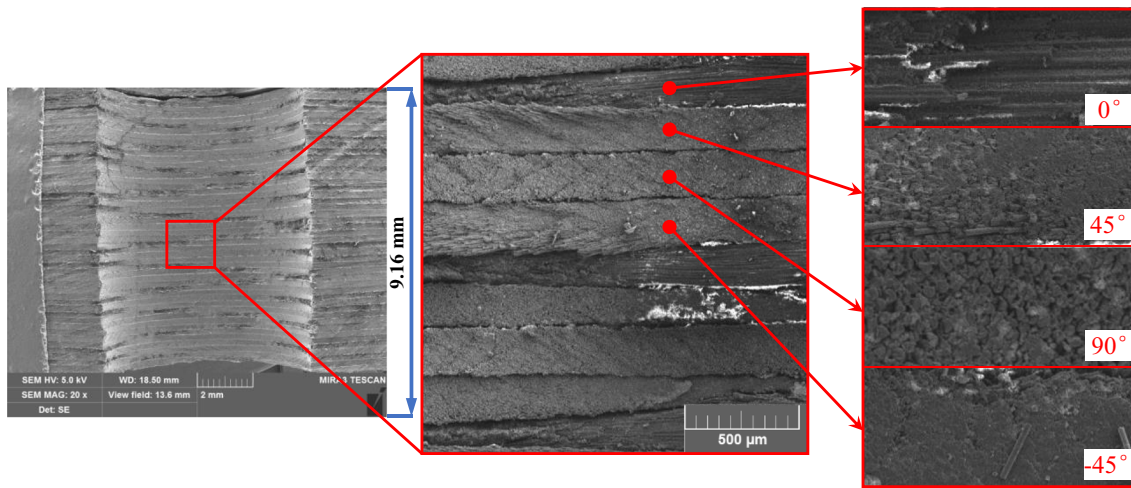
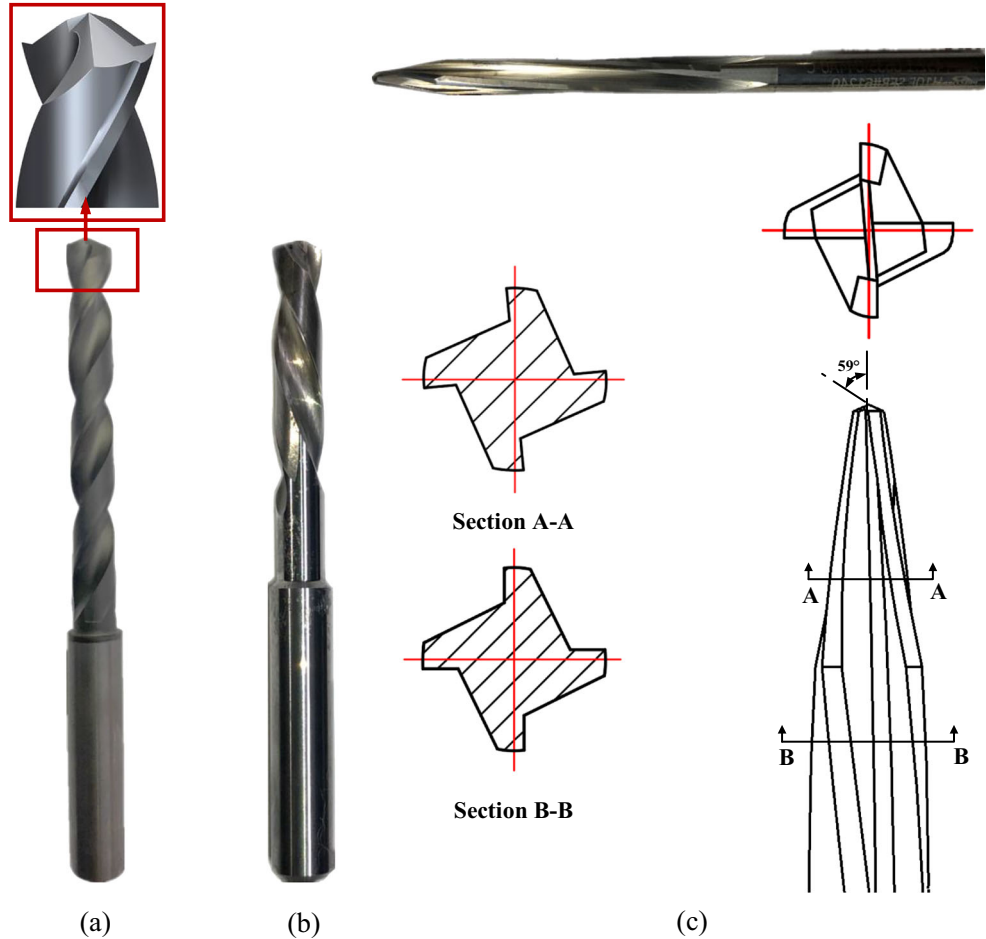


Fig. 2 SEM images of a hole cross-section showing the stacking sequence of the studied high-strength CFRP laminate

Each measure was repeated three times in order to get reliable results. Finally, the worn surface morphologies of drills were inspected using both SEM and EDS with the aim to identify the dominant wear mechanisms and failure modes. The effectiveness of different drill bits was evaluated and compared in terms of drilling forces, surface morphologies, hole quality, and wear behavior.

Fig. 3 Geometrical features of drill bits used for drilling high-strength CFRPs: brad spur drill (a), twist drill (b), and dagger drill (c)



3 Results and discussion

3.1 Analysis of the drilling forces

A fundamental step in understanding the drilling mechanics of CFRP composites is the investigation of cutting forces which contain important information related to the quality of holes

Table 1 Details of the experimental conditions for the drilling of T800/X850 laminates

	Level 1	Level 2	Level 3	Level 4
Spindle speed (n , rpm)	1000	1500	2000	2500
Feed rate (f , mm/rev)	0.010	0.015	0.020	0.025

and the wear of drills. Signals of thrust forces in the time domain with respect to different drill bits are shown in Fig. 4 for the case corresponding to $n = 2500$ rpm and $f = 0.025$ mm/rev. The thrust force commonly signifies the tribological interactions at the tool-work interface toward the feed direction, being an influential parameter determining the extents of interlaminar delamination. High fluctuations of thrust force signals are noted in the stable cutting zone except at the hole entry and exit sides due to the cyclic chip separation process of the carbon/epoxy system and the dynamic varying chip removal modes due to the changes of the fiber cutting angle. Moreover, it is noted that the brad spur drill produces the lowest magnitudes of thrust forces among drills tested due to its functionally designed edge geometries and the superior diamond coating against the rubbing of hard and abrasive carbon fibers while machining.

Additionally, both the brad spur drill and the twist drill exhibit similar variations of thrust force signals with the drilling time. As the drill approaches the workpiece (see stage A in Fig. 4), the chisel edge makes contact with the composite and results in a rapid increase of thrust force owing to its rubbing and plowing effects. However, the brad spur drill produces thrust forces experiencing a much slower increasing rate compared with the twist drill due to its functionally designed drill tip structure favoring the minimization of drilling forces. For both drills, the maximum magnitudes of thrust forces are reached when the conical part shape of the drills fully enters the interior of the sample and the drill tip is facing the sample bottom. Stage C for brad spur drill and twist drill appears when the chisel edge moves outside the bottom

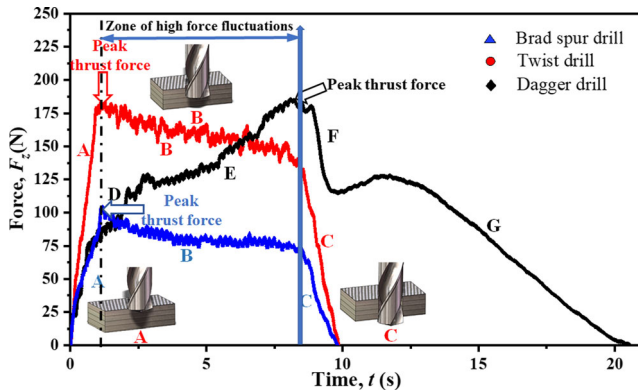


Fig. 4 Characterization of the thrust force signals in the time history during the drilling of high-strength CFRP composites with different drill bits ($n = 2500$ rpm and $f = 0.025$ mm/rev)

surface of the CFRP laminate where the thrust force decreases gradually as the cutting lips come out of the hole.

With respect to the dagger drill, the entry region of thrust force in the recorded time duration is featured by two different slopes due to the double point angles involved. Stages D and E signify the engagement of the first and second point angle drill lips within the CFRP laminate. The thrust force variation in the entry regions indicates the influence of the drill tip angles on the drilling forces. It is noticeable that the thrust force experiences a dramatic increase in stage D while it rises slowly in stage E due to the decrease in the point angle of the drill lips. The maximum thrust force appears at the end of stage E when the drill lips of the second point angle are fully engaged in the workpiece where the risk of interlaminar delamination is expected higher as the last plies of materials are pushed out by the chisel edge. After a short while, the magnitudes of the thrust force start to decrease dramatically as the drill lips come out of the hole and the reaming flutes enter the workpiece. Finally, the reaming process starts in stage G, where the drilling operation has finished and the drill bit begins reaming the hole to its final size. Problems occurring in this stage are related to the final size and finishing of the composite hole as the reaming is more likely to induce vibrations and chattering than drilling due to the reduced stiffness of the drill bit/workpiece system [18].

Figure 5 shows the effects of the drilling parameters on the magnitudes of thrust forces for each drill bit when machining the high-strength CFRP laminates. For both the brad spur drill and the twist drill, there is a clear elevation in the thrust force due to the increase in the spindle speed. The phenomenon is contrary to the findings observed in most experimental studies of drilling CFRP composites where the drilling thrust decreases with the increment of the spindle speed. A reasonable explanation is such that the elevated drilling temperatures due to the increased spindle speeds under the tested parametric range exert a negligible effect on the softening of the carbon/epoxy system. In the case of the dagger drill, the spindle speed affects the values of the thrust forces but fails to show a clear variation trend as evidenced in Fig. 5c. For all the drills examined, a linearly increasing correlation between the thrust force and the feed rate is identified due to the elevated cross section of chips while drilling CFRP composites. Under the tested drilling parameters, the brad spur drill produces the lowest thrust forces followed by the twist drill and dagger drill due to its large point angle and the superior diamond coating that reduces the friction at the tool-work interface. However, the dagger drill is found to promote the highest thrust forces even compared with the twist drilling of T800/X850 composites as depicted in Fig. 5.

3.2 Characterization of the drilled composite hole surfaces

The formation of the composite hole surfaces is closely related to the chip separation mode governed by the fiber cutting

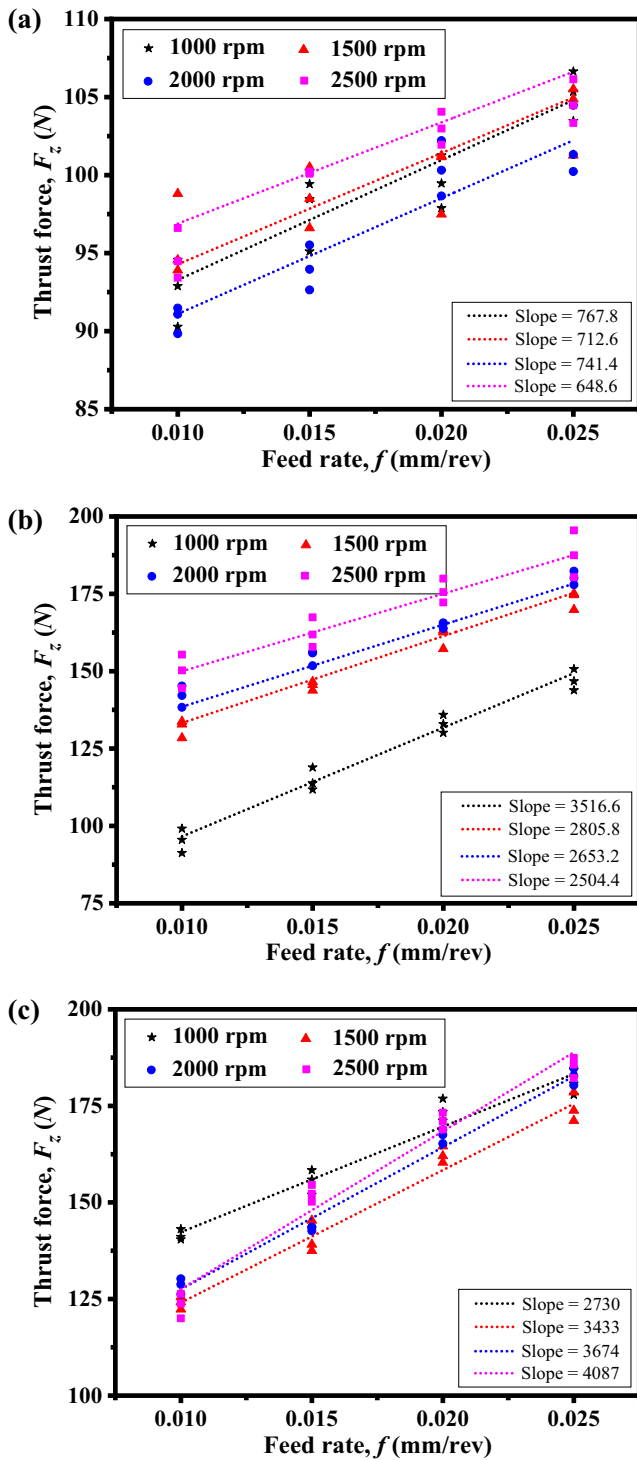


Fig. 5 Impact of the drilling parameters (spindle speed (n) and feed rate (f)) on the maximum thrust forces produced by the brad spur drill (a), the twist drill (b), and the dagger drill (c) during the drilling of high-strength CFRPs

angle as denoted in Fig. 6. Different types of fiber removal processes associated with the laminate orientations and drill geometrical features determine the final cut surfaces and the subsequent hole defects. Figures 7, 8, 9, 10, 11, and 12 present the surface morphologies of CFRP holes produced by three

drill bits under different cutting conditions. In general, the brad spur drill produces the smoothest hole surfaces with fewest defects compared with the twist drill and dagger drill under all the examined cutting conditions. The damage modes residing within the cut surfaces for the brad spur drill are featured by quantities of matrix smearing and re-deposited materials. Additionally, interlaminar delamination characterized by the debonding failure among adjacent plies of carbon fibers occurs almost at the hole exit side as shown in Fig. 7 due to the action of the feed force which pushes away the laminae directly under the drill tip being exceeding the critical thrust force. Increasing the spindle speed or decreasing the feed rate tends to exacerbate the extents of melted matrix smearing, which is possible due to the increased friction at the tool-work interface or the elevated tool-work interaction time resulting in the higher interface temperatures. The poor thermal conductivity of the carbon/epoxy composite was also a contributory factor in relation to the resin melt. The re-deposited materials onto the cut composite surfaces are mostly the debris of fiber dust or the residual resin formed due to the high pressures/temperatures at the tool-work interface. For all the drilling parameters investigated, the middle part of the cut hole surfaces for the brad spur drill basically remains intact without visible cavities or cracking even under the unfavorable fiber cutting angle of -45° as shown in Figs. 7 and 8.

In regard to the conventional twist drills, the cut hole surfaces are featured by various types of defects formed even at the low feed rates and low spindle speeds. Observations show that the interlaminar cracking among adjacent plies of carbon fibers due to the loss of supporting matrix becomes very prevalent in zones with the fiber cutting angle of -45° . Delamination during the twist drilling is identified to take place mainly at the hole exit side, which is consistent with the inspection for the case of using a brad spur drill. Surface cavities are characterized by the step-like morphologies exposing the fiber pullouts under the conditions of $n =$

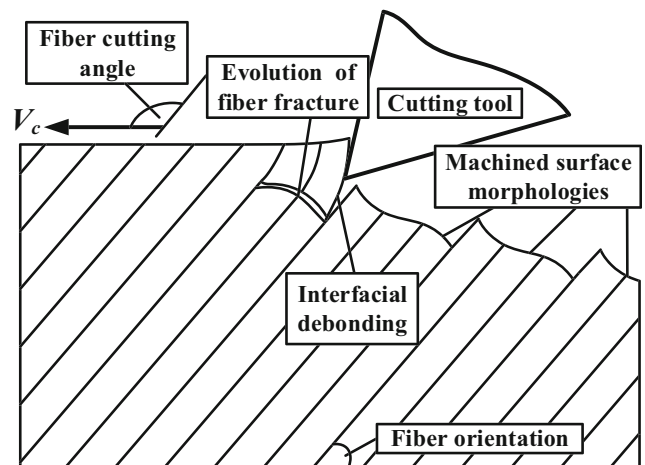


Fig. 6 Schematic illustration of the fiber cutting angle in the machining of a fibrous composite laminate

Cutting conditions	SEM morphologies	
$n = 1000$ rpm $f = 0.020$ mm/rev		
$n = 1500$ rpm $f = 0.020$ mm/rev		
$n = 2000$ rpm $f = 0.020$ mm/rev		
$n = 2500$ rpm $f = 0.020$ mm/rev		

Fig. 7 SEM morphologies of the CFRP holes produced by the brad spur drill under different spindle speeds

1500 rpm and $f = 0.020$ mm/rev in Fig. 9. The phenomenon is mainly caused by the bending-induced fracture which leads to the poorly cut fiber surfaces. Besides, the SEM analysis

reveals that the debris of bent and fractured fibers adhering onto the drilled composite holes is randomly formed while the phenomenon of the matrix smearing seems insignificant for all

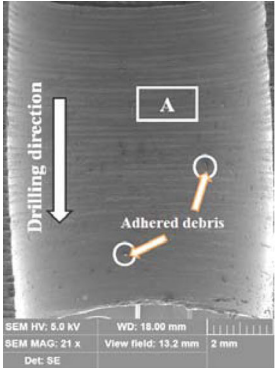
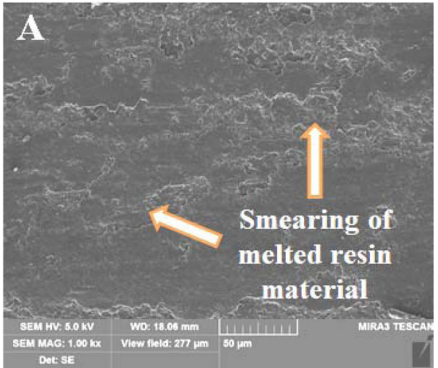
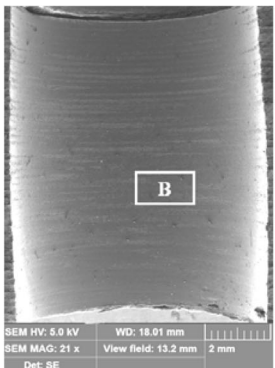
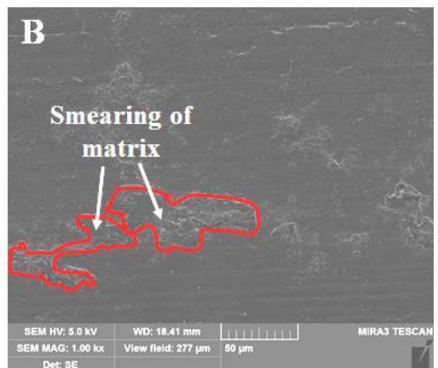
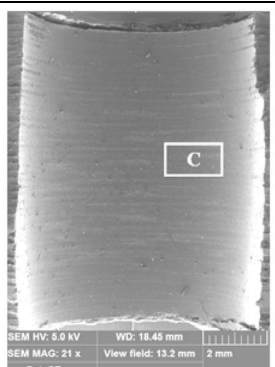
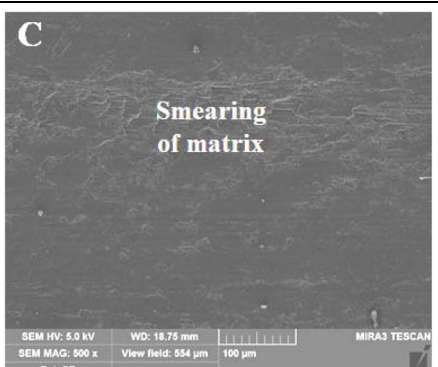
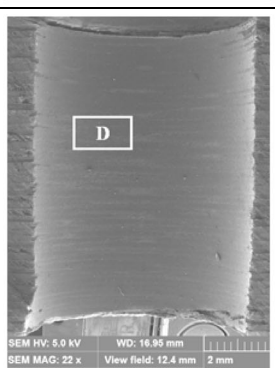
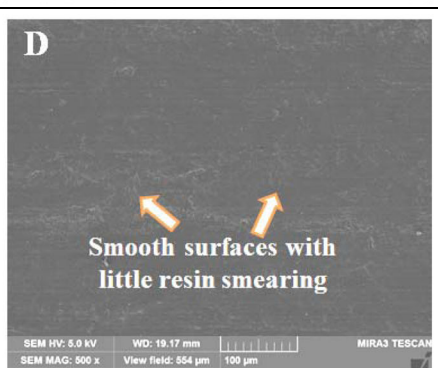
Cutting conditions	SEM morphologies	
$n = 2500$ rpm $f = 0.010$ mm/rev		
$n = 2500$ rpm $f = 0.015$ mm/rev		
$n = 2500$ rpm $f = 0.020$ mm/rev		
$n = 2500$ rpm $f = 0.025$ mm/rev		

Fig. 8 SEM morphologies of the CFRP holes produced by the brad spur drill under different feed rates

the cutting cases of the twist drill. Since increasing either the spindle speed or the feed rate could lead to the higher thrust forces (ref. Fig. 5b), both parameters affect adversely the

surface quality of the composite holes by the evidence that the area of the drilling-induced damage increases with the rise of spindle speeds and feed rates.

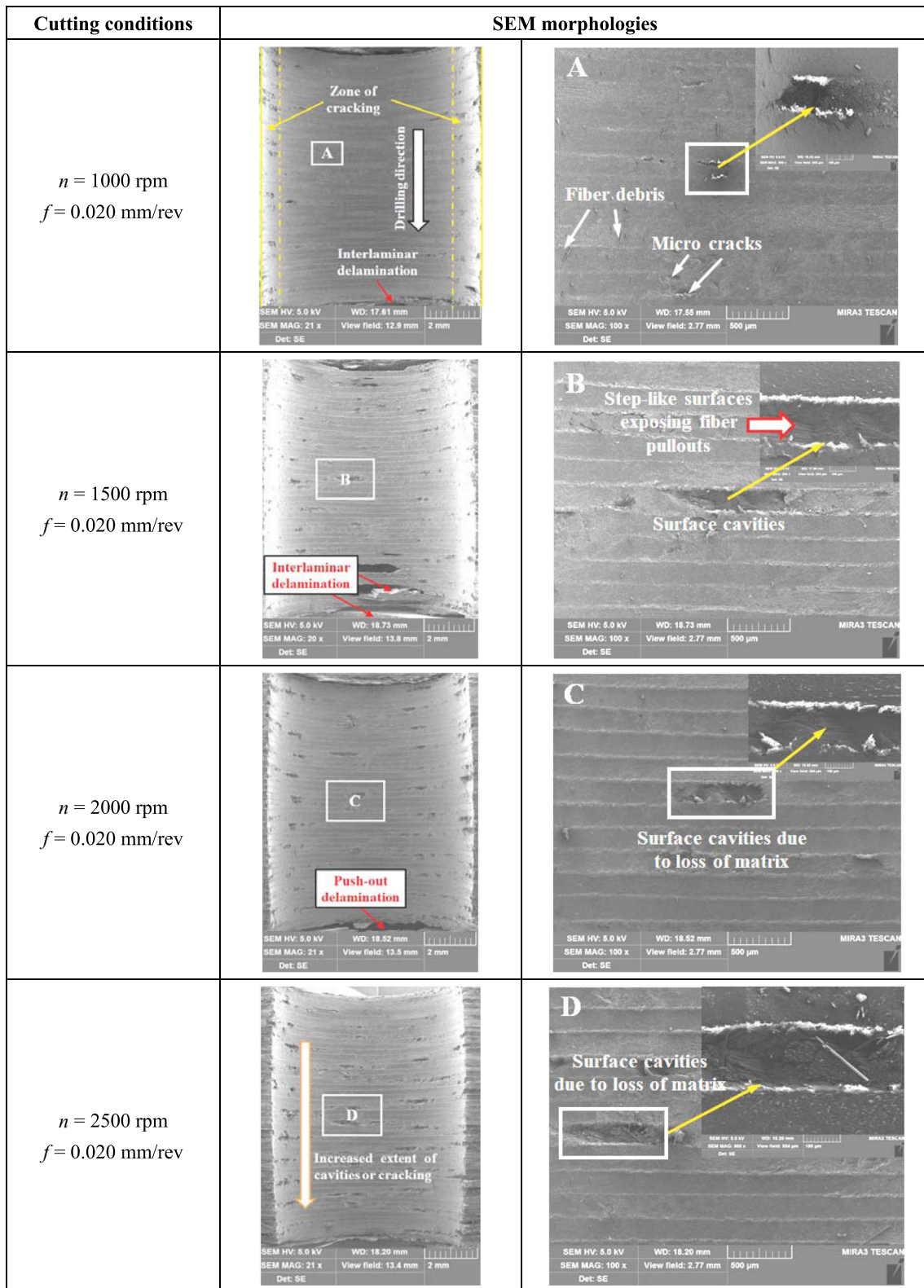


Fig. 9 SEM morphologies of the CFRP holes produced by the twist drills under different spindle speeds

As for the dagger drills, the cut CFRP hole surfaces are the poorest with a large amount of drilling-induced damage including fiber fractures, microcracking, push-out delamination,

resin adhesion, and fuzzing as depicted in Figs. 11 and 12. Interlaminar cracking is clearly visible between adjacent plies through the SEM examinations of drilled holes. Severe

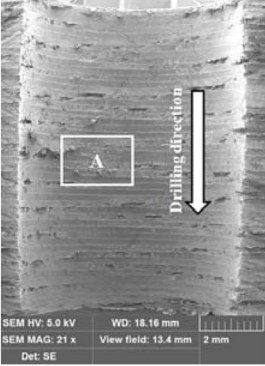
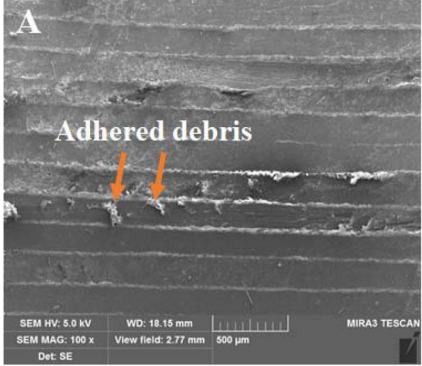
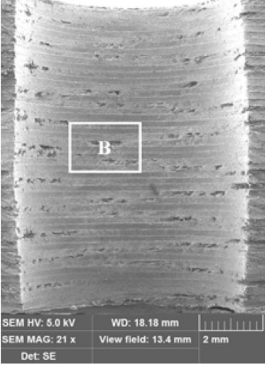
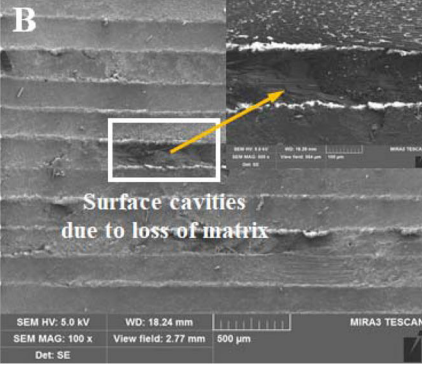
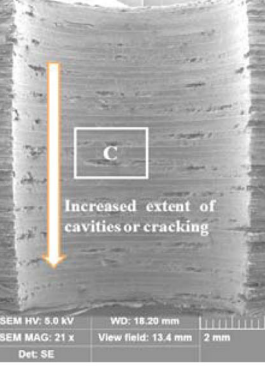
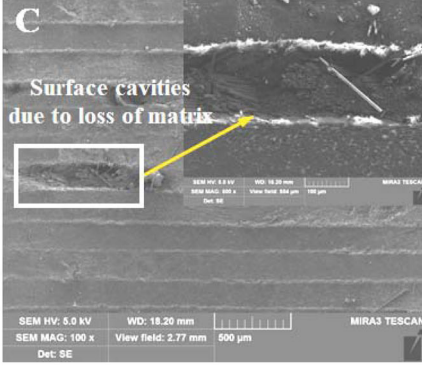
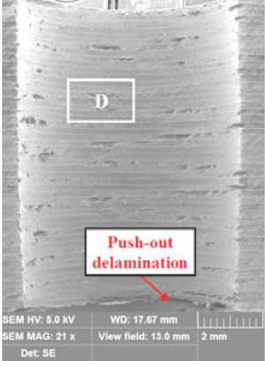
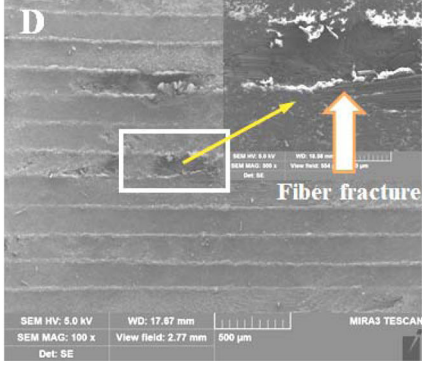
Cutting conditions	SEM morphologies	
<p>$n = 2500$ rpm $f = 0.010$ mm/rev</p>		
<p>$n = 2500$ rpm $f = 0.015$ mm/rev</p>		
<p>$n = 2500$ rpm $f = 0.020$ mm/rev</p>		
<p>$n = 2500$ rpm $f = 0.025$ mm/rev</p>		

Fig. 10 SEM morphologies of the CFRP holes produced by the twist drills under different feed rates

extrusion between adjacent plies due to the uneven load transfer between layers is observed in the case of $n = 2500$ rpm and $f = 0.010$ mm/rev, resulting in a certain degree of inter-layer

deformation. Smearing of the separated composite matrix and fiber debris onto the surface of the machined hole is pronounced near the hole exit side due to the rise of cutting

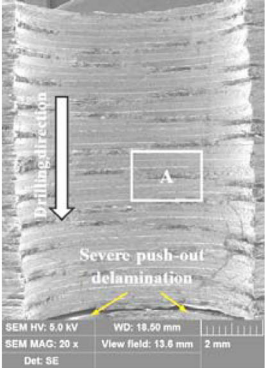
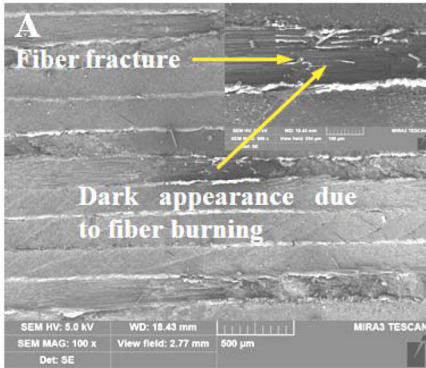
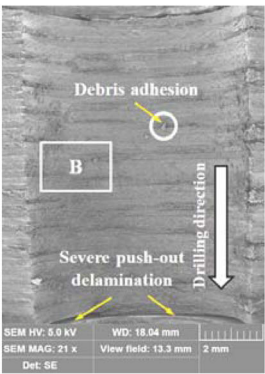
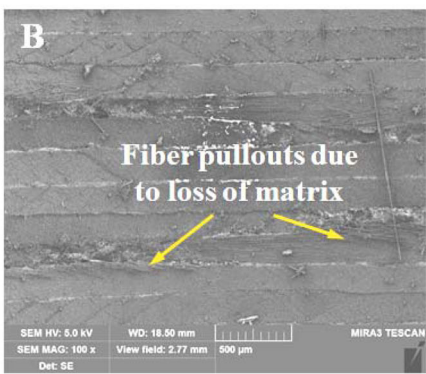
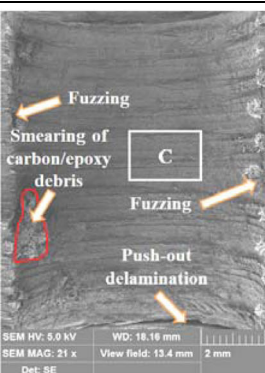
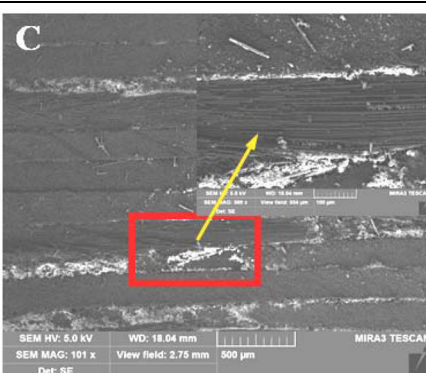
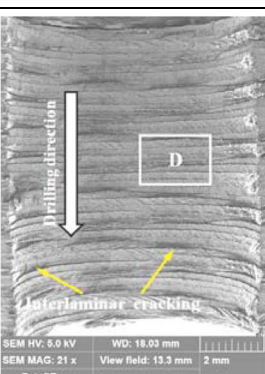
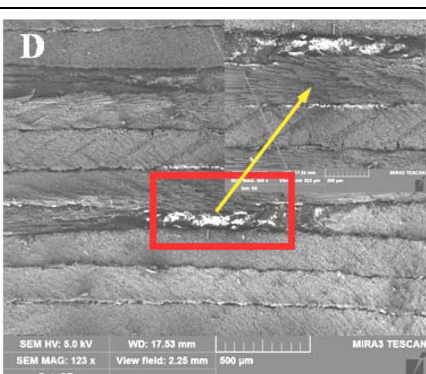
Cutting conditions	SEM morphologies	
<p>$n = 1000$ rpm $f = 0.020$ mm/rev</p>	 <p>Drilling direction</p> <p>Severe push-out delamination</p> <p>SEM HV: 5.0 kV WD: 18.50 mm SEM MAG: 20 x View field: 13.6 mm 2 mm Det: SE</p>	 <p>A</p> <p>Fiber fracture</p> <p>Dark appearance due to fiber burning</p> <p>SEM HV: 5.0 kV WD: 18.43 mm SEM MAG: 100 x View field: 2.77 mm 500 μm MIRA3 TESCAN Det: SE</p>
<p>$n = 1500$ rpm $f = 0.020$ mm/rev</p>	 <p>Debris adhesion</p> <p>Severe push-out delamination</p> <p>Drilling direction</p> <p>SEM HV: 5.0 kV WD: 18.04 mm SEM MAG: 21 x View field: 13.3 mm 2 mm Det: SE</p>	 <p>B</p> <p>Fiber pullouts due to loss of matrix</p> <p>SEM HV: 5.0 kV WD: 18.50 mm SEM MAG: 100 x View field: 2.77 mm 500 μm MIRA3 TESCAN Det: SE</p>
<p>$n = 2000$ rpm $f = 0.020$ mm/rev</p>	 <p>Fuzzing</p> <p>Smearing of carbon/epoxy debris</p> <p>Push-out delamination</p> <p>SEM HV: 5.0 kV WD: 18.16 mm SEM MAG: 21 x View field: 13.4 mm 2 mm Det: SE</p>	 <p>C</p> <p>SEM HV: 5.0 kV WD: 18.04 mm SEM MAG: 101 x View field: 2.75 mm 500 μm MIRA3 TESCAN Det: SE</p>
<p>$n = 2500$ rpm $f = 0.020$ mm/rev</p>	 <p>Drilling direction</p> <p>Interlaminar cracking</p> <p>SEM HV: 5.0 kV WD: 18.03 mm SEM MAG: 21 x View field: 13.3 mm 2 mm Det: SE</p>	 <p>D</p> <p>SEM HV: 5.0 kV WD: 17.53 mm SEM MAG: 123 x View field: 2.25 mm 500 μm MIRA3 TESCAN Det: SE</p>

Fig. 11 SEM morphologies of the CFRP holes produced by the dagger drills under different spindle speeds

temperatures with the drilling depth. The inspections of the magnified views of the hole morphologies indicate that the poorly cut surfaces for the dagger drill often reside within plies

having a -45° fiber orientation being featured by quantities of exposed fibers with a minimal degree of residual resin materials while neatly cut surfaces fully covered with matrix are

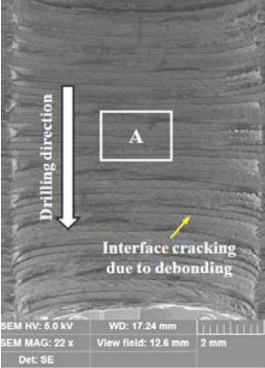
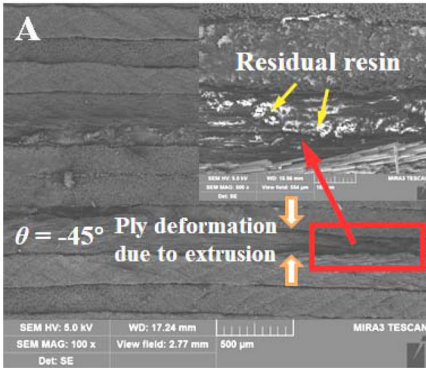
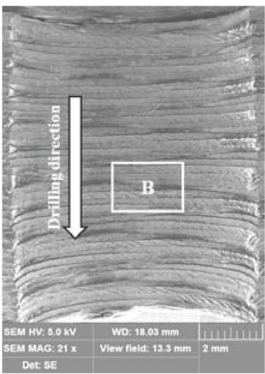
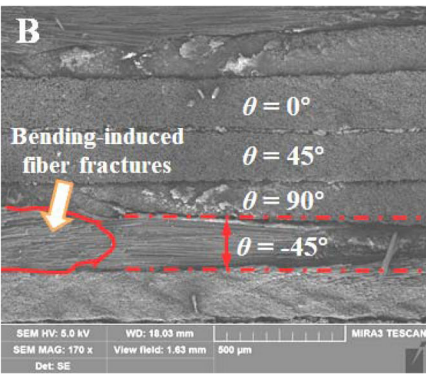
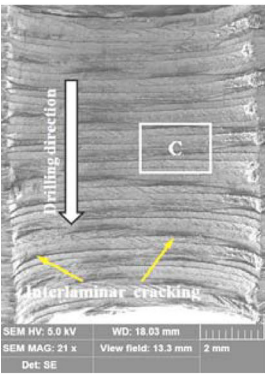
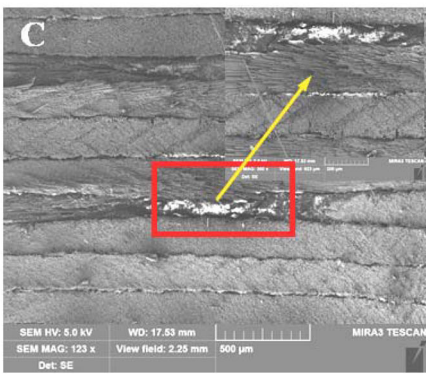
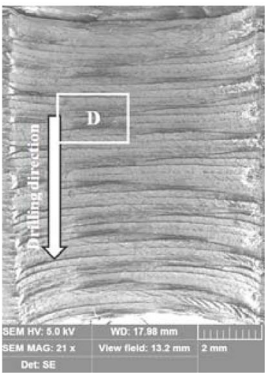
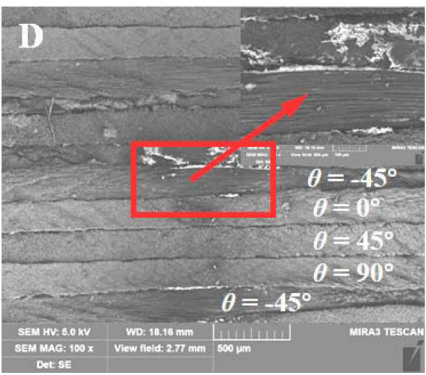
Cutting conditions	SEM morphologies	
<p>$n = 2500$ rpm $f = 0.010$ mm/rev</p>		
<p>$n = 2500$ rpm $f = 0.015$ mm/rev</p>		
<p>$n = 2500$ rpm $f = 0.020$ mm/rev</p>		
<p>$n = 2500$ rpm $f = 0.025$ mm/rev</p>		

Fig. 12 SEM morphologies of the CFRP holes produced by the dagger drills under different feed rates

mainly located at the 0° , 45° , and 90° plies as shown in Fig. 12. The phenomenon is due to the out-of-plane shear fracture along the fiber/matrix interface accompanied by

severe macro deformation induced by the bending pressure from the drill cutting edges for the case of -45° fiber orientation. Moreover, under the conditions of higher spindle

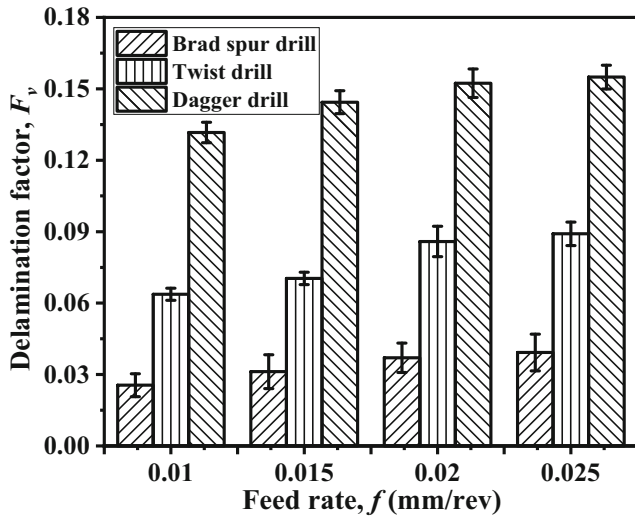


Fig. 13 Comparison of the delamination factor (F_v) for different drills under varying feed rates ($n = 2500$ rpm) [17]

speeds or higher feed rates, the surface quality of the CFRP holes tends to be considerably deteriorated with large amounts of damaged or imperfect areas visible on the hole surfaces. This implies a negative impact of the drilling parameters on the composite surface finish and suggests a combination of low spindle speeds and low feed rates benefiting the damage-free drilling of the high-strength CFRP laminates.

3.3 Quantification of the drilling-induced delamination damage

The severity of the interlaminar delamination was quantitatively analyzed since it affects significantly the structural integrity and long-term reliability of fibrous composite parts. Figure 13 shows the comparison of the three-dimensional

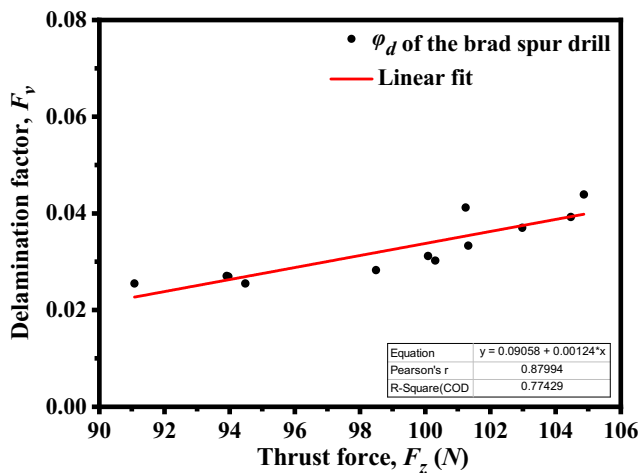


Fig. 14 Correlation between the thrust force and the three-dimensional delamination factor (F_v) for the brad spur drill when drilling high-strength CFRPs. (Note that the symbol x denotes the thrust force and the symbol y signifies the delamination factor)

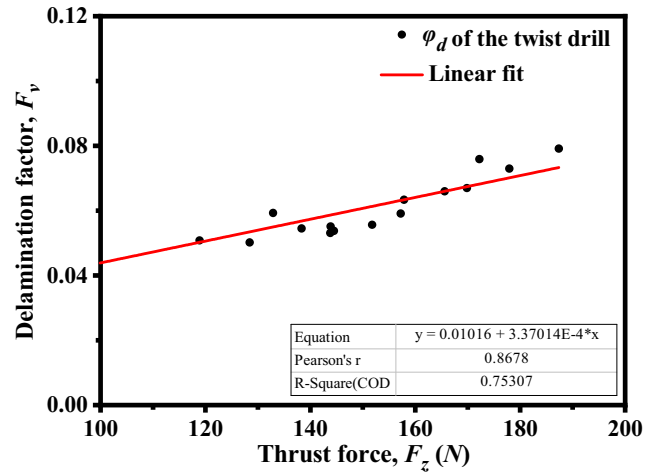


Fig. 15 Correlation between the thrust force and the three-dimensional delamination factor (F_v) for the twist drill when drilling high-strength CFRPs. (Note that the symbol x denotes the thrust force and the symbol y signifies the delamination factor)

delamination factor gained by different drill bits under varying feed conditions. It is clear that the extents of the drilling-induced delamination show a high sensitivity to the input feed rate as well as the drill geometries. Increasing the feed rate tends to significantly aggravate the severity of the delamination damage. The brad spur drill is confirmed to yield the best performance leading to the lowest levels of the 3D delamination factors due to its lowest thrust force generation followed by the twist drill and dagger drill (ref. Fig. 13 [17]). Moreover, the correlations between the thrust forces and the delamination factors for various drills tested are plotted in Figs. 14, 15, and 16. Note that the linear fitting results are also given in the three figures, where the symbol x denotes the thrust force and the symbol y signifies the delamination factor. It is apparent that the thrust force affects directly the extents of the cutting-

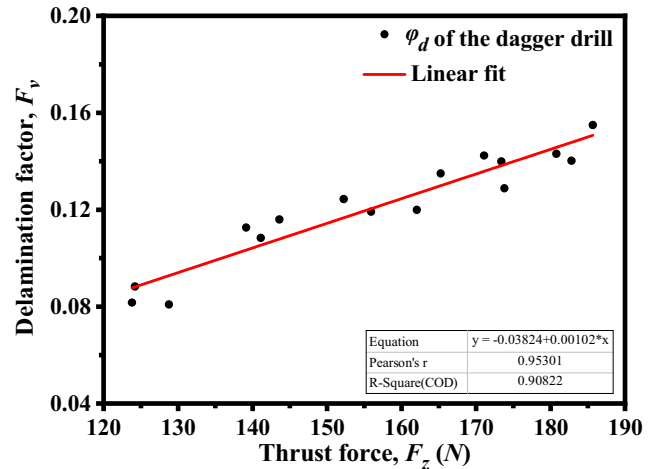


Fig. 16 Correlation between the thrust force and the three-dimensional delamination factor (F_v) for the dagger drill when drilling high-strength CFRPs. (Note that the symbol x denotes the thrust force and the symbol y signifies the delamination factor)

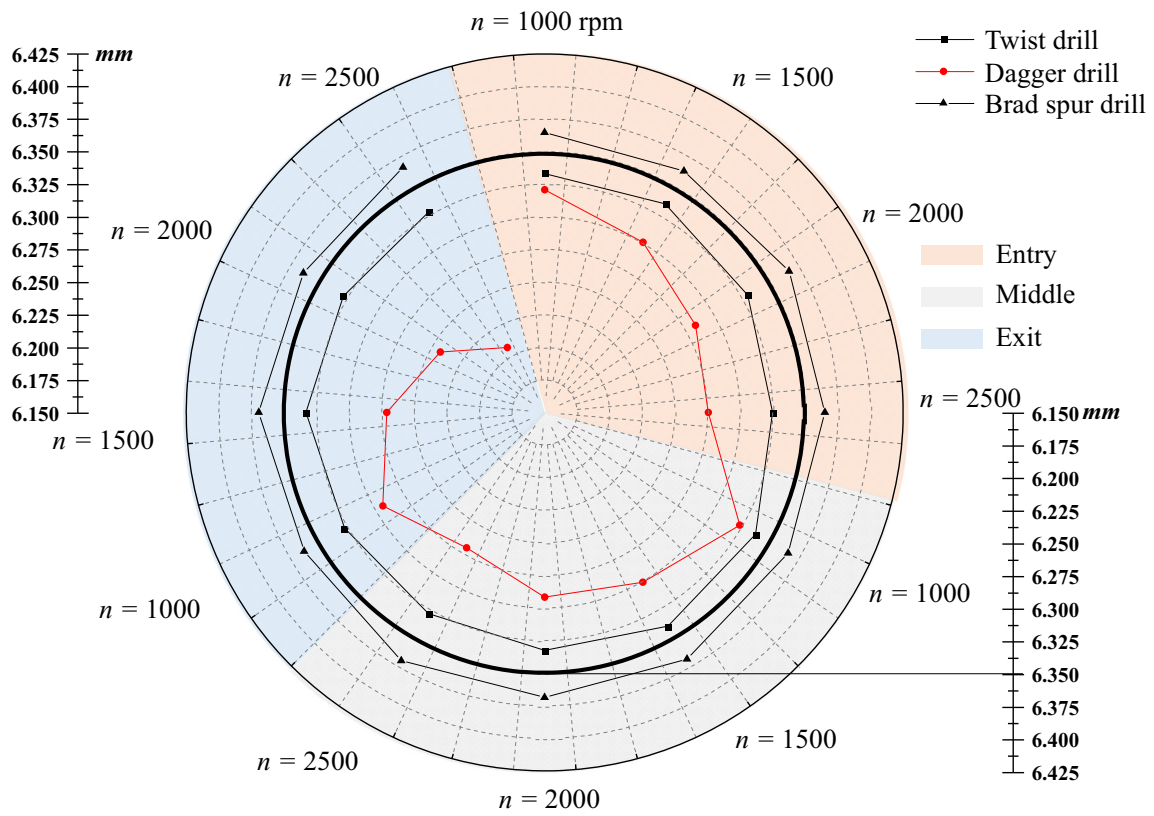


Fig. 17 Effect of the spindle speed (n) on the hole diameters produced by different drills after drilling high-strength CFRPs ($f=0.025$ mm/rev)

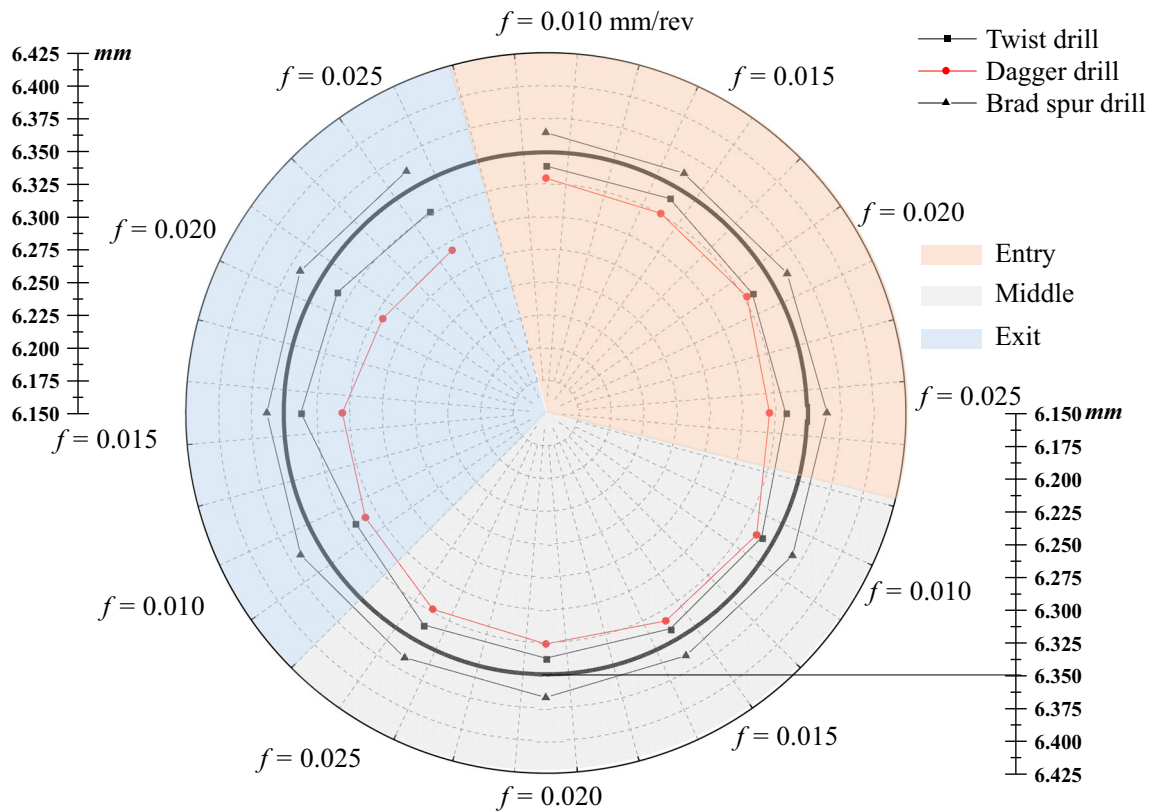


Fig. 18 Effect of the feed rate (f) on the hole diameters produced by different drills after drilling high-strength CFRPs ($n=1000$ rpm)

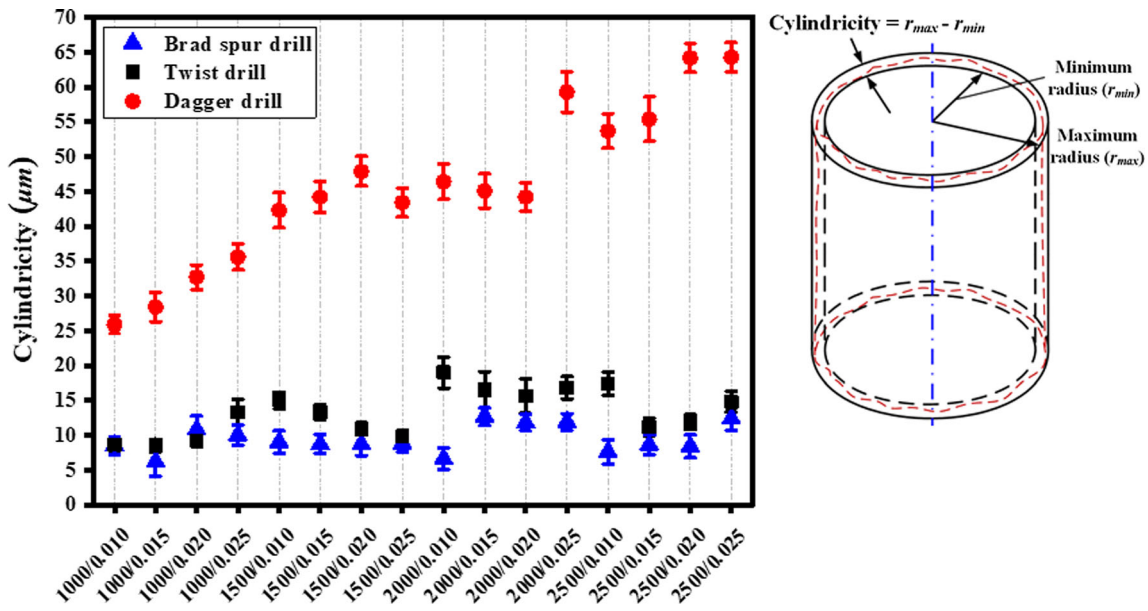


Fig. 19 Comparison of hole cylindricity errors obtained by various drills after drilling high-strength CFRPs

induced delamination, approximately showing a linearly increasing trend with the delamination factors. To calculate the critical thrust force (CTF) for each drill used, the method of linear fitting was utilized to correlate the data of delamination factors with the drilling thrust. The estimated CTFs for the brad spur drills, twist drills, and dagger drills after linear fitting are respectively 73.05 N, 30.15 N, and 37.49 N, which indicate that the brad spur drills retain the best capability to realize the delamination-free drilling of high-strength T800/X850 CFRP composites.

3.4 Assessment of the hole dimensional accuracy

Hole dimensional accuracy including the hole diameters and cylindricity was carefully addressed since it affects greatly the post assembly tolerance of drilled composite structures. Figures 17 and 18 show the obtained results of hole diameters under varying conditions. Note that measurements of the composite hole diameters were conducted at three regions located at the entry side, the middle side, and the exit side. Results indicate that the brad spur drill exhibits the best

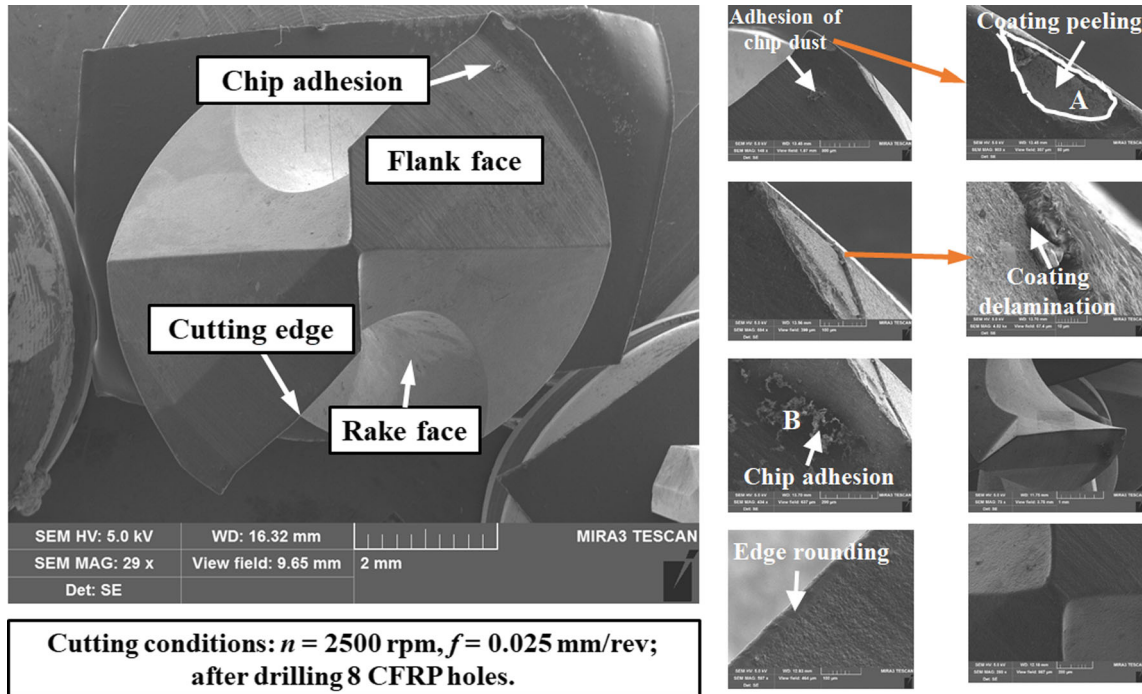


Fig. 20 SEM images of the worn surface morphologies for the brad spur drill after drilling high-strength CFRPs

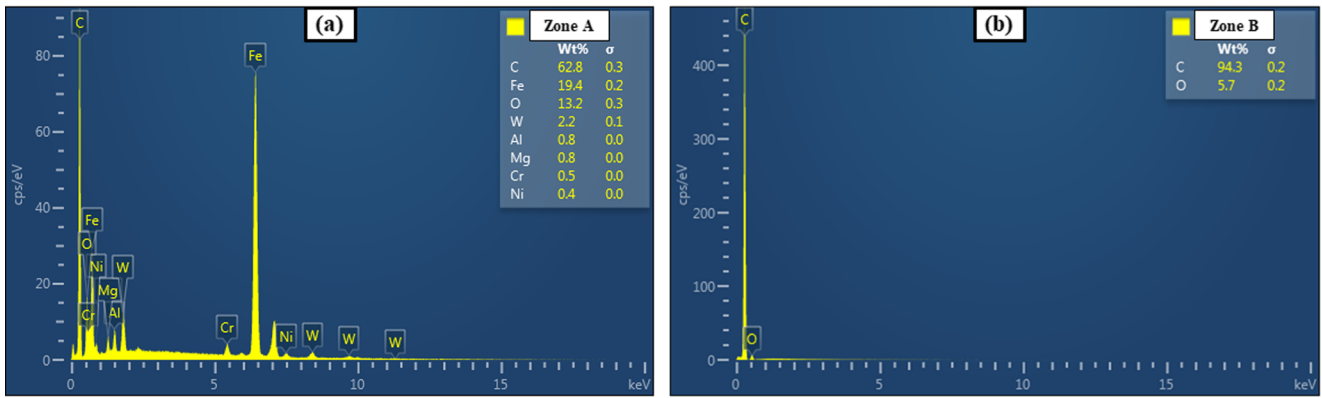


Fig. 21 EDS analysis of the chemical elements of the brad spur drill surfaces in Fig. 20: zone A (a) and zone B (b)

performance in guaranteeing a tight tolerance of CFRP hole diameters compared with the other two drills irrespective of the used cutting conditions. This is attributed to the functionally designed drill tip structures characterized by two protruding edges that assist in drilling centering, in preventing the extrusion effects of the chisel edge, and in minimizing the hole defects. Additionally, both the twist drill and dagger drill produced undersized CFRP holes with a high deviation to the nominal hole diameter. In most cases, the hole diameters measured in three regions for the brad spur drill seem to be independent of the input spindle speed and feed rate while diameters of holes produced by the twist drill and dagger drill tend to be highly affected by the input drilling parameters. For all conditions tested, diameters of holes measured at the exit side appear to deviate far from the nominal hole diameter for both the twist drill and dagger drill due to the

serious drilling-induced defects particularly the burrs of carbon fibers concentrated at the hole exit side. With respect to the results of hole cylindricity given in Fig. 19, the dagger drill often promotes the largest magnitudes of cylindricity for all the drilling parameters examined. The brad spur drill and the twist drill are also found to produce approximately the comparable magnitudes of hole cylindricity within the range of 5–20 μm and the drilling parameters do not show a clear impact on the variation of cylindricity for the CFRP holes.

3.5 Inspection of the tool wear modes

Machining fibrous composites entails rapid wear progression of tools and short tool life due to the highly abrasive nature of the reinforcing fibers. Most studies [3, 5, 11, 19, 20] dealing

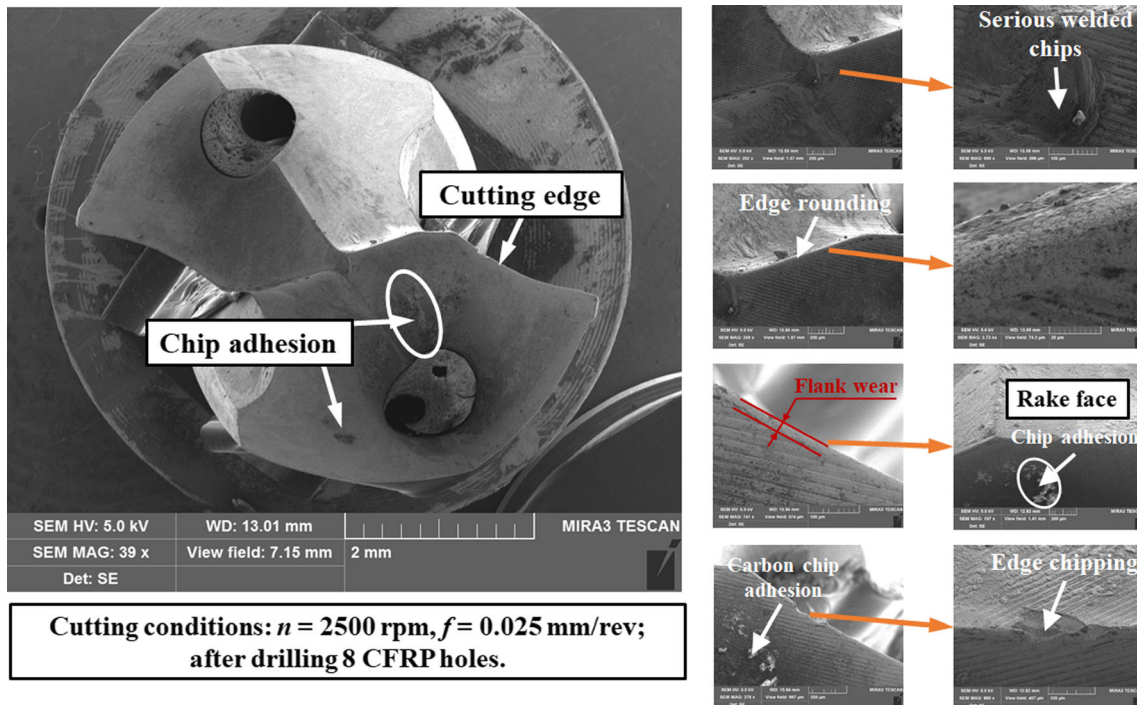


Fig. 22 SEM images of the worn surface morphologies for the twist drill after drilling high-strength CFRPs

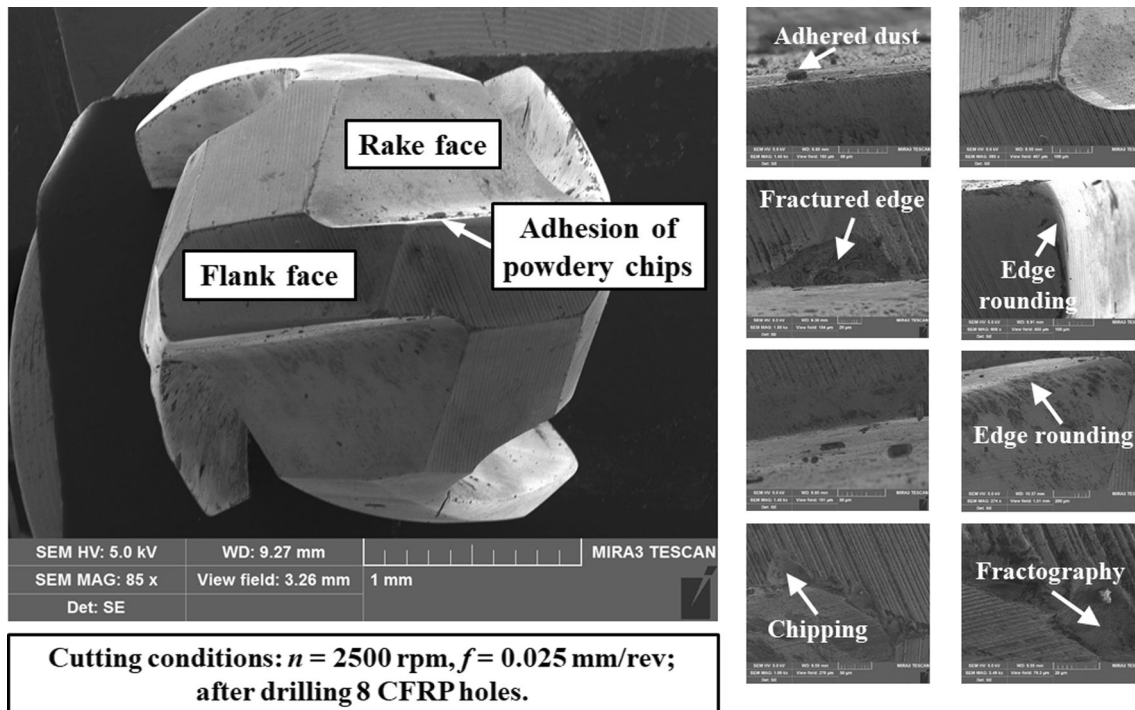


Fig. 23 SEM images of the worn surface morphologies for the dagger drill after drilling high-strength CFRPs

with the drilling of conventional low-strength CFRPs revealed that abrasive wear leading to the aggressive cutting edge rounding and the fracturing/chipping of drill edges are the key wear modes governing the tool wear process. In this subsection, SEM inspections of various worn drill surfaces were conducted in order to figure out the dominant wear mechanisms and failure modes while drilling the high-strength CFRP laminates. Figures 20, 21, 22, and 23 show the recorded SEM morphologies of the worn tool surfaces after drilling eight CFRP holes under the fixed cutting conditions of $n = 2500$ rpm and $f = 0.025$ mm/rev.

It is evident that the brad spur drill experiences a very negligible level of edge rounding, thanks to the high wear resistance of the diamond coating in alleviating the severe rubbing effects of the reinforcing fibers. Additionally, the lowest extent of adhesion of powdery carbon chips is identified onto the drill flank surface through the SEM examination. The phenomenon is mainly attributed to the high thermal conductivity of the diamond coating in reducing the cutting temperatures promoted at the tool-work interface. As shown in the magnified view of region A in Fig. 20, a partial cutting edge of the brad spur drill was catastrophically chipped due to the occurrence of coating peeling exposing the tool substrate surface, which is confirmed by the high content of elements of the tungsten carbide through the EDS analysis of the examined region (ref. Fig. 21). Further, delamination of the diamond coating along the cutting edges is identified which is mainly caused by the overload of the fatigue stresses during the composites drilling.

In contrast, both the twist drill and the dagger drill are found to suffer aggressive abrasion wear and adhesion wear after the drilling of high-strength CFRPs. As depicted in Fig. 22, the twist drill is observed to be welded firmly by a large area of powdery fiber dust along the drill chisel edge. In addition, the flank wear and edge rounding due to fiber abrasions are found to dominate the wear progression of the twist drill. Adhesion of fiber dust onto the flank surface is also identified and the edge chipping is confirmed as the key failure mode of the twist drill due to the tungsten carbide being brittle in nature that is unable to sustain high stresses and thus undergoes chipping [5]. With regard to the dagger drill, the tool exhibits the weakest ability in resisting the aggressive wear arising from the high-strength CFRP drilling process. Similar to the wear behavior of the conventional twist drill, the dagger drill commonly suffers a much greater extent of edge rounding and edge fracturing even after drilling eight CFRP holes as evidenced in Fig. 23. Both abrasion wear and adhesion wear are identified as the main wear patterns for the dagger drill and edge fracture/chipping operates as the key drill failure mode.

4 Conclusions

The present paper contributes to an experimental investigation into the drilling characteristics of high-strength T800/X850 CFRPs representative of aircraft components. The novelty of this work lies in identifying the feasibility of using different

specialized drills in improving the machinability of the high-strength CFRP. Various drilling responses including the drilling forces, hole morphologies, workpiece damage, hole dimensional accuracy, and tool wear were precisely addressed with respect to the used process parameters and the drill bits. The results indicate that drilling high-strength CFRP laminates entails various types of thermally and mechanically induced damage of hole wall surfaces involving the interlaminar delamination, matrix smearing, cracking/cavities, and chip adhesion. The wear mechanisms of drilling high-strength CFRP composites are abrasive wear leading to the edge rounding of drills and adhesion wear due to powdery chip welding, while the key tool failure modes are coating peeling or edge chipping. The brad spur drill is confirmed to yield the best performance followed by the twist drill and the dagger drill in terms of drilling forces, hole quality, and tool wear behavior. The results highlight the importance of developing a functionally designed drill bit as well as the excellent match between the tool material and the composite workpiece in achieving the damage-free drilling of high-strength CFRP composites.

Funding information The authors gratefully acknowledge the financial support of the National Natural Science Foundation of China (Grant No. 51705319), Shanghai Pujiang Program (Grant No. 17PJ1403800), and Shanghai Academy of Spaceflight Technology (Grant No. SAST2017-060). The work is also partly sponsored by the Research Project of State Key Laboratory of Mechanical System and Vibration (Grant No. MSVZD201704).

References

- Karpat Y, Değer B, Bahtiyar O (2012) Drilling thick fabric woven CFRP laminates with double point angle drills. *J Mater Process Technol* 212(10):2117–2127
- Anand RS, Patra K (2017) Mechanistic cutting force modelling for micro-drilling of CFRP composite laminates. *CIRP J Manuf Sci Technol* 16:55–63
- Gaugel S, Sripathy P, Haeger A, Meinhard D, Bernthaler T, Lissek F, Kaufeld M, Knoblauch V, Schneider G (2016) A comparative study on tool wear and laminate damage in drilling of carbon-fiber reinforced polymers (CFRP). *Compos Struct* 155:173–183
- Malhotra SK (1990) Some studies on drilling of fibrous composites. *J Mater Process Technol* 24:291–300
- Rawat S, Attia H (2009) Wear mechanisms and tool life management of WC-Co drills during dry high speed drilling of woven carbon fibre composites. *Wear* 267(5–8):1022–1030
- Faraz A, Biermann D, Weinert K (2009) Cutting edge rounding: an innovative tool wear criterion in drilling CFRP composite laminates. *Int J Mach Tools Manuf* 49(15):1185–1196
- Wang X, Kwon PY, Sturtevant C, Kim D, Lantrip J (2013) Tool wear of coated drills in drilling CFRP. *J Manuf Process* 15(1): 127–135
- Shyha IS, Aspinwall DK, Soo SL, Bradley S (2009) Drill geometry and operating effects when cutting small diameter holes in CFRP. *Int J Mach Tools Manuf* 49(12–13):1008–1014
- Sorrentino L, Turchetta S, Bellini C (2018) A new method to reduce delaminations during drilling of FRP laminates by feed rate control. *Compos Struct* 186:154–164
- Loja MAR, Alves MSF, Bragança IMF, Rosa RSB, Barbosa ICJ, Barbosa JI (2018) An assessment of thermally influenced and delamination-induced regions by composites drilling. *Compos Struct* 202:413–423
- Fernández-Pérez J, Cantero J, Díaz-Álvarez J, Miguélez M (2017) Influence of cutting parameters on tool wear and hole quality in composite aerospace components drilling. *Compos Struct* 178: 157–161
- Díaz-Álvarez A, Rodríguez-Millán M, Díaz-Álvarez J, Miguélez MH (2018) Experimental analysis of drilling induced damage in aramid composites. *Compos Struct* 202:1136–1144
- Qiu X, Li P, Li C, Niu Q, Chen A, Ouyang P, Ko TJ (2018) Study on chisel edge drilling behavior and step drill structure on delamination in drilling CFRP. *Compos Struct* 203:404–413
- Geier N, Szalay T, Takács M (2019) Analysis of thrust force and characteristics of uncut fibres at non-conventional oriented drilling of unidirectional carbon fibre-reinforced plastic (UD-CFRP) composite laminates. *Int J Adv Manuf Technol* 100(9):3139–3154
- Abrão AM, Faria PE, Rubio JCC, Reis P, Davim JP (2007) Drilling of fiber reinforced plastics: a review. *J Mater Process Technol* 186(1–3):1–7
- Liu D, Tang Y, Cong WL (2012) A review of mechanical drilling for composite laminates. *Compos Struct* 94(4):1265–1279
- Xu J, Li C, Mi S, An Q, Chen M (2018) Study of drilling-induced defects for CFRP composites using new criteria. *Compos Struct* 201:1076–1087
- Fernandes M, Cook C (2006) Drilling of carbon composites using a one shot drill bit. Part I: five stage representation of drilling and factors affecting maximum force and torque. *Int J Mach Tools Manuf* 46(1):70–75
- Wang X, Kwon PY, Sturtevant C, Kim D, Lantrip J (2014) Comparative tool wear study based on drilling experiments on CFRP/Ti stack and its individual layers. *Wear* 317(1–2):265–276
- Çelik A, Lazoglu I, Kara A, Kara F (2015) Wear on SiAlON ceramic tools in drilling of aerospace grade CFRP composites. *Wear* 338:11–21

Publisher's note Springer Nature remains neutral with regard to jurisdictional claims in published maps and institutional affiliations.